Are the shoreline and eutrophication of desert lakes related to desert development?

Lihui Luo [a,b], Wenzhi Zhao [a,b*], Lixin Wang [c*], Igor Ogashawara [c,d], Qiyue Yang [a,b], Hai Zhou [a,b], Rong Yang [a,b], Quntao Duan [a,b], Chenglin Zhou [e], Yanli Zhuang [a,b,c]

[a] Linze Inland River Basin Research Station, Key Laboratory of Inland River Basin Ecohydrology, Northwest Institute of Eco-Environment and Resources, Chinese Academy of Sciences, Lanzhou 730000, China

[b] University of Chinese Academy of Sciences, Beijing 100049, China

[c] Department of Earth Sciences, Indiana University-Purdue University Indianapolis (IUPUI), Indiana 46202, USA

[d] Department of Experimental Limnology, Leibniz-Institute of Freshwater Ecology and Inland Fisheries, Stechlin 16775, Germany

[e] Lanzhou Information Center, Northwest Institute of Eco-Environment and Resources, Chinese Academy of Sciences, Lanzhou 730000, China

Corresponding author:

*E-mail: zhaowzh@lzb.ac.cn & lxwang@iupui.edu

ORCID

Lihui Luo: 0000-0002-9471-7373

Wenzhi Zhao: 0000-0003-1757-226X

Lixin Wang: 0000-0003-0968-1247

Igor Ogashawara: 0000-0001-6328-0001

Chenglin Zhou: 0000-0003-1486-4371

This is the author's manuscript of the article published in final edited form as:

Luo, L., Zhao, W., Wang, L., Ogashawara, I., Yang, Q., Zhou, H., Yang, R., Duan, Q., Zhou, C., & Zhuang, Y. (2021). Are the shoreline and eutrophication of desert lakes related to desert development? Environmental Monitoring and Assessment, 193(1), 43. https://doi.org/10.1007/s10661-020-08806-0

Abstract

Desert lakes are unique ecosystems found in oases within desert landscapes. Despite the numerous studies on oases, there are no reports regarding the spatiotemporal distribution and causes of eutrophication in the desert lakes that are located at the edge of the Linze Oasis in northwestern China. In this study, the seasonal shoreline and eutrophication of a desert lake were monitored using an unmanned aerial vehicle (UAV) and water sampling during three crop growth stages. The spatial extents of the shoreline and algal blooms and the chromophoric dissolved organic matter (CDOM) absorption coefficient were derived through UAV images. The desert lake shoreline declined during the crop growing stage, which exhibited the largest water demand, and began to expand after this stage. The estimated CDOM absorption coefficient measurements and classified algal bloom area showed seasonal variations that increased from spring to late summer and then decreased in autumn. The first two crop growth stages accounted for most of the water and fertilizer requirements of the entire growth period, which may have contributed to large amounts of groundwater consumption and pollution and resulted in peak eutrophication of the lake in the second growth stage. However, the CDOM absorption coefficient of the third stage was not well correlated with that of the first two stages, suggesting that the lake may be affected by the dual effects of groundwater and precipitation recharge in the third stage. These results indicate that the water quality of desert lakes may be affected by agricultural cultivation. The agricultural demands for water and fertilizer may change the spatiotemporal changes in water quality in the lake, especially in the middle and early stages of crop growth.

Keywords: Desert lake; Desert development; Unmanned aerial vehicle; Shoreline; Eutrophication; Algal blooms

1. Introduction

Lakes are important aquatic environments that provide a variety of ecosystem services (Creutz et al. 2016; Steinman et al. 2017). However, problems such as anthropogenic eutrophication are a serious threat to their ecological functioning (Cluis et al. 1988; Jin et al. 2005; Le et al. 2010). A desert lake is a unique yet threatened ecosystem and a natural landscape in arid and semiarid regions; however, desert lakes are distinguished as rare water bodies in desert oases (Ojwang et al. 2016; Wen et al. 2014). Desert lakes cover only a small proportion of the desert landscape, but they have an irreplaceable ecological effect and significance for local residents, animals and plants (Fathi and Flower 2005). The expansion and sustainability of oases and desert blooming require a tremendous amount of groundwater resources, pesticides and fertilizers. Groundwater is often the most important source of water for oasis agriculture, where precipitation is scarce, surface water sources are absent, and evaporation far exceeds precipitation (Chang et al. 2015; Chen et al. 2016). Thus, groundwater plays an important role in the process of water resource circulation in desert oases (Chen et al. 2004). Meanwhile, groundwater is an important source of recharge for desert lakes.

Anthropogenic lake eutrophication is predominantly caused by human activities, which discharge large amounts of residue into lakes from industrial wastewater, domestic sewage, farmland fertilization and pesticides through runoff and groundwater, resulting in a rapid increase in the contents of nutrients, such as nitrogen and phosphorus (Daryanto et al. 2017). Dissolved organic matter (DOM) is considered to

be the largest reservoir of organic carbon in water bodies (Benner and Biddanda 1998). Currently, chromophoric dissolved organic matter (CDOM), as a part of DOM, has been extensively studied in terms of its role in ecology (Heller et al. 2016; Song et al. 2019; Valerio et al. 2018). The distributions of CDOM and algal blooms represent fundamental indicators of the eutrophication status of inland lakes (Zhang et al. 2018). CDOM is very common in aquatic environments, affecting the optical properties of water columns and regulating the metabolism and traceability of biogeochemical cycles (Song et al. 2019; Zhang et al. 2018). Fluorescent dissolved organic matter (fDOM) refers to the portion of the large CDOM pool that emits fluorescence, and fDOM serves as a quick and easy way to track DOM in natural waters. CDOM absorbs light from the ultraviolet and visible wavelengths and partially emits the absorbed light as fDOM. The absorption of CDOM will further affect the growth of plankton communities and affect aquatic ecosystems (Heller et al. 2016). There is growing interest in the observation of algal blooms and CDOM in water bodies via remote sensing since it can assess the spatial distribution of both parameters. However, appropriate spectral wavelengths and fine spatial resolutions are required for the remote spatial assessment of small lakes (Dörnhöfer and Oppelt 2016). When the environmental carrying capacity of a lake is exceeded, a large number of algal blooms may occur under the appropriate light and water temperature conditions (Brooks et al. 2016; Duan et al. 2009). A serious consequence of algal bloom outbreaks is the deterioration of water quality (Wells et al. 2015). In addition to eutrophication, the water level of desert lakes is an important

factor driving aquatic ecosystem changes. The regular fluctuation of the water levels will lead to shoreline changes (Templin et al. 2017).

Agricultural cultivation is the most important human activity contributing to desert development. Desert oases are dominated by sandy soils; thus, pesticide and fertilizer residues can easily enter groundwater from sandy soil, which in turn pollutes the groundwater (Binding et al. 2018; Luo et al. 2020). As a result of the expansion and sustainability of oases, algal blooms and water pollution have increased due to additional nutrient inputs into aquatic systems (Chen et al. 2016). The reclamation and sustainability of oases have increased eutrophication and other environmental problems after ecosystem disruption (Su et al. 2010; Yang et al. 2016). It is important to explore the interrelationship between algal biomass and water quality to understand the ecological sensitivity of desert lakes. Satellite remote sensing imagery provides an effective solution for monitoring the dynamics of algal blooms and CDOM (Brezonik et al. 2015). However, for small lakes, the spatial resolution or pixel size of most satellite sensors is too coarse to observe these water bodies. Therefore, remote sensing based on unmanned aerial vehicles (UAVs) may be an alternative method for collecting data at high spatial resolutions at reduced costs (Luo et al. 2018; Peter et al. 2014; Wu et al. 2019).

Aquatic ecosystems represent a complex phenomenon that is dynamic in both space and time (Li et al. 2018). Currently, there is little research on the eutrophication of desert lakes. The study of lake eutrophication in turn reveals the impact of agriculture

on the surrounding groundwater and lakes. To further understand the impacts of agricultural cultivation on the shoreline, water quality, and algal bloom changes in a desert lake, we chose a typical lake in a desert-oasis ecotone to the south of the Badain Jaran Desert, China, and studied its seasonal environmental changes. The objectives of this study are to 1) detect the seasonal water quality changes and map algal bloom distributions using a portable water quality monitoring instrument and UAV, 2) analyze the spatiotemporal variations in lake area, water quality and algal blooms during different crop growing stages, and 3) assess the driving forces of the spatiotemporal trends in water quality and algal bloom changes.

2. **Materials and Methods**

2.1. Study area

Suolongtan Lake (100°7′55″E, 39°22′5″N) is a freshwater desert lake located at the edge of Linze Oasis in northwestern China, and the Badain Jaran Desert lies to the north of the Linze Oasis (Figure 1). The elevation is approximately 1250 m, and the groundwater is shallow, with a mean depth of approximately 2 m. The lake has a surface area of 0.11 km^2 and a shoreline of 1.7 km. Common reeds, which overgrow the lake's edges and form islands towards the middle of the lake, are a valuable habitat for a number of birds. This lake has experienced constant changes in response to both anthropogenic and natural hydrological forcing. Groundwater and precipitation dominate the water level changes in the lake at different times. However, because of

the high seepage of sandy land, there is very little surface runoff. Thus, the lake depends on groundwater discharge for most of its freshwater inflow. The water from the lake is a source of irrigation for oasis crops; therefore, there are significant but unmeasured irrigation abstractions from a pump (Figure 2).

Since the 1960s, the sandy land around the lake has been gradually reclaimed for agriculture (Xie et al. 2017). Agriculture has always been the most important human activity around this lake. There are water conservancy facilities near farmland, including wells and canals. The function of water wells is mainly to extract groundwater, and canals transport groundwater and surface water. The major ground cover types around the lake include maize, *Haloxylon* forest, bare soil, and dirt roads, with small regions of other short vegetation. The study area has an arid climate, which is cold in winter and hot and dry in summer. The average annual temperature is 7.6 °C. The annual total precipitation is approximately 120 mm, of which 65% is mainly distributed in summer as short-term showers, while the average annual potential evaporation is approximately 2400 mm, which is 20 times greater than the annual total precipitation (Zhao and Chang 2014). The precipitation, evaporation and groundwater table data came from a weather station 0.69 km from the lake. The precipitation at the end of August and the beginning of September is the greatest, and the largest evaporation occurs between June and July. The groundwater shows a trend of first falling and then rising throughout the year, with the turning point at the end of July and early August (Figure 3).

The croplands of the Linze Oasis account for more than 41% of the total oasis area, and the crops are mainly maize. The Linze Oasis is developed in the Gobi Desert, and the sand content of the soil is very high (61%). The sand soil has a weak water-holding capacity, high infiltration rate and low fertility. The water and fertilization requirements of crops are much larger than those of other soil types. The mean water requirement during the growth period is 500-600 mm, but the actual irrigation is approximately 800 mm because of the desire to obtain high crop yields (Su et al. 2014). The expansion and sustainability of the oasis has accelerated the extraction of groundwater. The maximum extraction of groundwater generally occurs between July and August. Agricultural water accounts for more than 90% of the total water use. In the growing season, the fertilization ratio of N, P and K is generally 1:0.48:0.26, and the mean fertilization amounts are 533.60 kg ha^{-1} for N, 214.77 kg ha^{-1} for P_2O_5, and 97.22 kg ha^{-1} for K_2O (Su et al. 2010). Local agriculture uses extensive fertilization management, and the actual amount of fertilization is generally higher than the amount of fertilizer required.

2.2. Water quality measurements

A water quality instrument (YSI® EXO1 Sonde) with four sensors was used for water quality monitoring (https://www.ysi.com/EXO1). Water quality parameters, such as conductivity, dissolved oxygen (DO), fDOM, pH, oxidizing-reducing potential (ORP) and salinity, were measured. The UAV and water quality sensor measurements were conducted in Suolongtan Lake between May 2018 and September 2018. After

each drone flight, the water quality was monitored again. The measured lake water depth did not exceed 30 cm. After each measurement, calibration solution was placed into a calibration cup equipped with a water quality instrument to calibrate the sensors. To avoid disturbing the aquatic birds living in the center of the lake, the water quality near the lake center was not sampled; however, sampling was extensive along the shoreline. The eastern region of the lake was difficult to access due to its deep depths; thus, there were few measurements from this area.

2.3. UAV flight experiment

UAV flights were performed using a DJI® Inspire 1 equipped with a Zenmuse X3 optical camera with a custom glare filter, which improves imaging in bright conditions. The camera has a resolution of 4000 by 3000 pixels and a focal length of 20 mm and acquired red-green-blue (RGB) images using this consumer-grade miniature UAV system. UAV flights were conducted between 10 a.m. and 2 p.m., with ambient light conditions ranging from full sunlight to partly cloudy conditions. A total of three drone flights and water quality sampling tests were deployed during three maize growing stages: maize flowering, mid-grain filling and maturation (Table 1). Flight operations were performed automatically using the Pix4Dcapture mobile application at an overlap of 80% and at 50 and 120 m above ground level, using the parallel strip method to fly to generate an imagery dataset. Multiple flights were conducted during each sampling,

and a total of 1644 photos were taken. The average ground sampling distance (GSD) ranged between 2.18 cm and 3.36 cm.

Images from the drone flights were stitched together into an OrthoMosaic using Agisoft® PhotoScan software (version 1.30); then, the shoreline of the lake and the distribution of algal blooms in the lake were extracted using a supervised classification procedure that combined edge detection methods using eCognition® Developer software (version 9.0). Classification first requires segmentation, setting the segmentation scale, and then classifying water bodies, vegetation and bare land; then, objects on the water are extracted, the water bodies are subdivided, the lake water, algae blooms, and grasses are classified, and finally islands are classified (Figure 4).

2.4. Mapping of the CDOM absorption coefficient

CDOM is optically measurable, making it an ideal choice for quantifying the water quality using remote sensing technology. The CDOM absorption coefficient can be used to characterize the optical properties of CDOM. Kutser et al. (2005) used the blue and green band ratios of Landsat satellite data to calculate the CDOM absorption coefficient in small lakes. The use of blue and green band ratios was considered to be a very successful application for CDOM estimation. Currently, no uniform remote sensing method is widely accepted for computing the CDOM absorption coefficient (Slonecker et al. 2016). To assess the seasonal CDOM trend of desert lakes, in this study, the absorption coefficient of CDOM was used as an indicator of the CDOM

concentration (Li et al. 2018; Valerio et al. 2018). The absorption coefficient of CDOM was modeled according to Eq. (1):

$$\alpha_{CDOM} = 5.20 * \left(\frac{Blue}{Green}\right)^{-2.76} \quad (1)$$

where blue and green are the blue (470 nm) and green (550 nm) bands of the UAV RGB imagery, respectively, and α_{CDOM} is the absorption coefficient of CDOM (m^{-1}) (Kutser et al. 2005).

To evaluate the remote estimation of the absorption coefficient of CDOM, we evaluated its relationship with fDOM measurements. Para et al. (2013) showed that the absorption coefficients of CDOM and fDOM have a strong linear correlation for Canadian coastal waters. This relationship was also observed in aquatic environments from Chile, New Zealand and the USA (Rose et al. 2014). Therefore, the fDOM values collected by the YSI® EXO1 Sonde were used to evaluate the remote estimation of the absorption coefficient of CDOM.

2.5. Statistical and principal component analysis

All statistical tests were performed using R statistical software. Analysis of variance (ANOVA) with Pearson tests and principal component analysis (PCA) were conducted using the FactoMineR and factoextra R packages to summarize the data for the parameters that control water quality and to evaluate the impacts of water quality at different crop growth stages. The ggplot2 R package was applied to plot the lake area changes, water quality changes, precipitation, evaporation and groundwater table. The

locally estimated scatterplot smoothing (LOESS) regression method was applied to fit the changing trend of the groundwater table. All spatial statistics and maps were generated by Esri ArcGIS software (version 10.2).

3. Results

3.1. Seasonal changes in lake shoreline

During the second growth stage, the water level declined by 1.04 m from that of the first stage, and then the water level increased by 2.46 m (Table 2). The lake areas and shorelines followed the same pattern. In the early and middle growth stages, crops require more water. The farmlands surrounding the desert lake rely on groundwater and lake irrigation, which causes a significant drop in the water level during the first two growth stages. After the second stage of crop growth, the water demand is sharply reduced. Thus, groundwater can recharge the lake, and the water level increases in the third stage.

3.2. Spatiotemporal dynamics of lake water quality

The average conductivity, fDOM, ORP and salinity were higher in the second growth stage (mid-grain filling) than in the prior (flowering) and following (maturity) growth stages (Table 2). However, the average DO showed an opposite trend, and the average pH values showed an increasing trend. The sample conductivity, as well as ORP and fDOM values, were significantly different ($p < 0.05$) in the three growth

stages. The DO and pH were significantly different ($p < 0.05$) between only the first two and third growth stages, and for salinity, there was no significant difference between the three stages.

PCA was conducted using the relative scores of the six water quality variables for all water samples to determine the degree of separation between the different crop growth stages (Figure 5). PCA detected high correlations among the six parameters, and the first two PCA axes contributed 86.1% of the variation in the six water quality variables, with Dim1 and Dim2 accounting for 57.8% and 28.3%, respectively. Furthermore, the results showed a general clustering of most water samples, with Dim1 scores ranging from −3 to 9 and Dim2 scores ranging from −3 to 4. The water samples in the mid-grain filling stage were generally scattered, with high Dim1 and Dim2 scores. In contrast, for the water samples in the flowering and maturity stages (scores ranging from −3 to 1 for Dim1 and from −2 to 3 for Dim2), the score distributions were clustered, and the Dim1 scores were low. The Dim1 and Dim2 PCA plots showed that conductivity and salinity were closely associated with fDOM and were negatively associated with pH and DO. PCA identified fDOM, salinity and conductivity as potential tracers of water chemical changes in the lake.

Because fDOM had a high dimension score, it could be used to demonstrate the spatiotemporal changes. The fDOM concentrations showed high spatial and temporal variability in the surface waters of Suolongtan Lake (Figure 6). The spatial difference in fDOM in different growth stages was high. The fDOM concentrations were highly

variable, ranging from 0.11 to 32.54 ppb QSE, and the fDOM variability in the second stage (relative standard deviation = 78%) also exceeded the variability in the other two stages (Table 2). The highest and lowest mean values of fDOM were recorded in the second and third stages, respectively, which suggests that the fDOM in the lake was the highest around July, the fDOM increased as the crops flowered, and the fDOM declined as crops approached maturity.

3.3. Spatiotemporal dynamics of the CDOM absorption coefficient

To evaluate the estimation of the absorption coefficients of CDOM, we used fDOM values to verify their relationship with the absorption coefficients of CDOM for the respective pixels in the UAV image (Figure 7). This analysis showed that the fDOM and the estimated CDOM absorption coefficients had a significant positive correlation ($P < 0.05$) and a strong correlation. The correlation coefficients (r) for the three stages were 0.85, 0.86 and 0.71. Based on this result, we believe that the absorption coefficient of CDOM could be estimated from the UAV images.

The spatial distribution of the simulated CDOM absorption coefficient in the three crop growing stages is illustrated in Figure 8. The lake water CDOM absorption levels displayed distinct spatial heterogeneity. The CDOM absorption coefficient was highest around the nearshore regions in the three stages. The simulated CDOM absorption coefficient first increased from the flowering stage and then decreased in the mid-grain filling stage (Figure 8 and Table 2). The CDOM absorption coefficients of the first and

second stages showed a significant negative correlation ($P < 0.05$, $R = -0.27$). In the maturity stage, the absorption coefficient and spatial difference in CDOM absorption were the smallest. Meanwhile, there was no significant correlation between the maturity stage and the first two stages.

3.4. Spatiotemporal dynamics of lake algal blooms

Algal blooms showed seasonal changes; specifically, blooms increased from spring to late summer and decreased in autumn (Figure 9). Algal blooms showed a trend of first increasing from the flowering stage and then decreasing in the mid-grain filling stage. The percent coverage ranged widely, which increased after the flowering stage (19% total area), peaked in the mid-grain filling stage (38% total area), and declined in the maturity stage (17% total area). From the perspective of spatial distribution, there were many algal blooms on the edges of the lake and islands, there were few blooms in the center of the lake, and there were many algal blooms in the northeastern part of the lake.

4. Discussion

4.1. Variations in lake shoreline and the driving factors

The water level is an important factor affecting the geomorphological parameters of lakes, and it fluctuates regularly, which leads to changes in the shoreline. In the exploration of the driving factors affecting the shoreline or changes in desert lake areas,

other studies and our studies have shown that farmland irrigation and evaporation are indeed two major factors causing seasonal variations in desert lakes (Habeck-Fardy and Nanson 2014). Therefore, precipitation and evaporation are generally selected as meteorological factors, and farmland irrigation is selected as a human activity factor for in-depth quantitative analysis. Although there are no monitoring data on crop irrigation in this study, the water demand characteristics of the crops in this study area at different growth stages are clear. Several studies have shown that the peak ecological water consumption for maize in manmade oases in this study area occurs in mid-June (Li et al. 2016; Zhao et al. 2010). Precipitation in the latter stage (from mid-grain filling to maturity, 66.6 mm) in the study area was significantly greater than that in the first stage (from flowering to mid-grain filling, 13.1 mm), but the evaporation in the early stage (686.5 mm) was greater than that in the latter stage (459.3 mm). Groundwater initially decreases and then increases at the end of July. These results suggest that the water demand of crops in the previous phase required increased irrigation from the groundwater and the lake. Because the precipitation in the latter period was much greater than that in the previous period and the evaporation was less than that in the previous period, we believe that the lake was affected by the dual effects of groundwater and precipitation in the third stage. As crop water demand and evaporation declined, the water level in the lake increased during the latter stage due to precipitation and groundwater recharge. The amount of water consumption by crops affects the length of the lake's shoreline, which was consistent with the changes in the lake shoreline

monitored by the UAV. These results also showed that precipitation played an important role in the short-term changes in the lake shoreline.

4.2. Lake eutrophication dynamics and the driving factors

Changes in the aquatic environment in oases are affected by a combination of natural and human-induced forces, as are the pollution and natural recovery processes of desert lakes (Souza et al. 2006). The water-holding capacity of sandy soils is lower than that of silt soil or clay. Oases are mainly made up of sandy soils, and pesticides and fertilizers are likely to seep down and contaminate the groundwater (Zhang et al. 2019). The use of fertilizers and pesticides on crops contributes to the accumulation of nutrients and toxic substances (i.e., bioaccumulation). Due to the lack of industries, settlements, or rivers around the lake, the sewage that enters the lake can be ignored. The elevation of cropland in the eastern and northern parts of the lake is higher than the elevation of the lake and other areas, so the eutrophication of the lake may be mainly affected by the cropland in the eastern and northern parts of the lake.

Before the mid-grain filling stage, in July, the proportion of maize fertilization in oases accounted for the majority of the total fertilization (Liu et al. 2017; Wang et al. 2010). Some studies have shown a significant positive correlation between the CDOM absorption coefficient and the trophic level of lakes (Song et al. 2019; Zhang et al. 2018). Both the first and second stages of the CDOM absorption coefficient showed a significant correlation, while the third stage was less relevant to the first two stages.

With the decrease in the CDOM absorption coefficient, the CDOM of the lake was stabilized, and the disturbance was minimal in the last stage. Through PCA, the degree of water quality dispersion in the second stage was the largest, which indicated that the spatial variability in water quality was highest in the second stage, especially for fDOM, salinity and conductivity. These results are consistent with the spatial distribution of the simulated CDOM absorption coefficient. Additionally, the external disturbances were most impactful in the second stage. Meanwhile, the seasonal changes in the fDOM, salinity and conductivity were highest in the second stage, which was related to crop fertilization and groundwater recharge. Clearly, fDOM and CDOM absorption within aquatic ecosystems was significantly affected by the groundwater sources of organic matter, which came from agricultural cultivation through groundwater (Yang and Liu 2010; Yang et al. 2016). These results showed that the simulated CDOM and observed fDOM conformed to the characteristics of the changes in DOM and indicated that the hydrologic cycle process in the third stage was not the same as that in the first two stages. This finding indicates that in addition to the influence of groundwater, other sources of water, such as rainfall in the third stage, may also have an impact on the eutrophication changes in the desert lake.

The overall trend of the CDOM absorption coefficient was consistent with that of algal blooms. The algal blooms and CDOM absorption coefficients showed opposite trends in terms of spatial distribution, and the CDOM absorption coefficient was largest in the regions with few algal blooms and vice versa (Figure 10). These results

demonstrated that algal blooms can cause increased concentrations of organic matter (Binding et al. 2018; Zhao et al. 2009). The study area experienced phytoplankton growth from July to September. CDOM is a nutrient needed for phytoplankton, and its growth is bound to consume a certain amount of CDOM. The photochemical degradation of CDOM leads to a decrease in CDOM in phytoplankton, which shows that CDOM and algal blooms exhibit opposite spatial distribution characteristics. Furthermore, the CDOM absorption coefficients showed a negative correlation in the first two stages. Similarly, Brezonik et al. (2005) observed that because algal blooms have higher radiation rates than CDOM in freshwater lakes, it is difficult to identify the CDOM levels in the water bodies during algal blooms. This result indicates that the water conditions are already at high fertility during the mid-grain filling stage. The algal blooms are in dire need of light penetration, phosphorus and nitrogen, which will affect the growth of algal blooms under high fertility (Brooks et al. 2016; Duan et al. 2009).

Despite the lack of monitoring data required for the calibration and quantification of the CDOM remote sensing method, the UAV-simulated CDOM absorption coefficient was able to retrieve the temporal and spatial variability in water chemical properties within the desert lake. These results indicate that groundwater recharges the desert lake and will be seasonally affected due to groundwater pollution and deterioration. In addition, fishing, lakeside barbecues and other human activities affect the eutrophication of desert lakes. The chemical properties of the water in desert lakes vary widely depending on the seasonal water level fluctuations, meteorological

conditions and growth stages of crops and can cause increased nutrients, leading to high levels of algal blooms and high spatiotemporal heterogeneity in aquatic ecosystems.

4.3. Uncertainties and future directions

Currently, satellite remote sensing data are often used to simulate the absorption coefficient of CDOM through the blue-green or blue-red band to extract the spatial distribution of algal blooms through classification, edge detection methods and bio-optical modeling, and there are few applications using UAVs. There are many uncertainties in both the simulation of the CDOM absorption coefficient and the extraction of algal blooms. The rapid development and application of UAVs and their sensors provide promising solutions and new opportunities for monitoring aquatic ecosystems. UAV-mounted multispectral or hyperspectral sensors may be a good solution to reduce the uncertainty of eutrophication parameterization in desert lakes (Kislik et al. 2018). Compared to the RGB band, sensors with more bands and high spectral resolutions will be able to better evaluate CDOM as well as chlorophyll-*a*. It is also necessary to combine UAVs, *in situ* monitoring and laboratory analysis to verify UAV remote sensing data, update the method used to simulate the CDOM absorption coefficient and improve the accuracy of algal bloom monitoring.

5. Conclusions

Desert lakes are very rare in the natural landscape. The joint testing and analysis of eutrophication in desert lakes based on sampling and UAVs has demonstrated that

seasonal changes in fDOM, salinity, conductivity, the estimated absorption coefficient of CDOM and algal blooms were strongly related to the agricultural cultivation of oases. The change in the lake shoreline exhibited a strong relationship with agricultural water consumption, while the seasonal dynamics of water quality and algal blooms were clearly related to the groundwater supply and precipitation linked to the use of fertilizers in different crop growth stages. The main source of water for desert lakes came from groundwater, and the hydrological and chemical cycles of groundwater affected the eutrophication level of desert lakes, which elucidates their impacts on the biogeochemistry of this unique aquatic ecosystem. The development of oases exerts a direct impact on the biogeochemical properties of unique desert lake aquatic ecosystems. The desert lake may, therefore, represent the chemistry pool in the oasis with seasonal variations in quality and quantity, which influence the degree and rate of eutrophication. Although the eutrophication of the lake is at a low level, the problem of human-induced eutrophication in desert lakes cannot be ignored as the development of the desert continues to advance.

Acknowledgements

This research was jointly supported by the National Key Research and Development Program of China (2019YFC0507400), the Key Research Project of Frontier Science of the Chinese Academy of Sciences (QYZDJ-SSW-DQC040), and the National Natural Science Foundation of China (41877545, 41871065). Lixin Wang

acknowledges partial support from the Division of Earth Sciences of National Science Foundation (NSF EAR-1554894) and the President's International Research Awards from Indiana University.

Conflicts of interest

The authors declare no competing financial interests.

References:

Benner, R., & Biddanda, B. (1998). Photochemical transformations of surface and deep marine dissolved organic matter: Effects on bacterial growth. *Limnology and Oceanography, 43*(6), 1373-1378. https://doi.org/10.4319/lo.1998.43.6.1373.

Binding, C. E., Greenberg, T. A., McCullough, G., Watson, S. B., & Page, E. (2018). An analysis of satellite-derived chlorophyll and algal bloom indices on Lake Winnipeg. *Journal of Great Lakes Research, 44*(3), 436-446. https://doi.org/10.1016/j.jglr.2018.04.001.

Brezonik, P., Menken, K. D., & Bauer, M. (2005). Landsat-based Remote Sensing of Lake Water Quality Characteristics, Including Chlorophyll and Colored Dissolved Organic Matter (CDOM). *Lake and Reservoir Management, 21*(4), 373-382. https://doi.org/10.1080/07438140509354442.

Brezonik, P. L., Olmanson, L. G., Finlay, J. C., & Bauer, M. E. (2015). Factors affecting the measurement of CDOM by remote sensing of optically complex inland waters. *Remote Sensing of Environment, 157*, 199-215. https://doi.org/10.1016/j.rse.2014.04.033.

Brooks, B. W., Lazorchak, J. M., Howard, M. D. A., Johnson, M.-V. V., Morton, S. L., Perkins, D. A. K., et al. (2016). Are harmful algal blooms becoming the greatest inland water quality threat to public health and aquatic ecosystems? *Environmental Toxicology and Chemistry, 35*(1), 6-13. https://doi.org/10.1002/etc.3220.

Chang, X., Zhao, W., & Zeng, F. (2015). Crop evapotranspiration-based irrigation management during the growing season in the arid region of northwestern China. *Environmental Monitoring and Assessment, 187*(11). https://doi.org/10.1007/s10661-015-4920-9.

Chen, D., Jin, G., Zhang, Q., Arowolo, A. O., & Li, Y. (2016). Water ecological function zoning in Heihe River Basin, Northwest China. *Physics and Chemistry of the Earth, Parts A/B/C, 96*, 74-83. https://doi.org/10.1016/j.pce.2016.08.005.

Chen, J. S., Li, L., Wang, J. Y., Barry, D. A., Sheng, X. F., Gu, W. Z., et al. (2004). Groundwater maintains dune landscape. *Nature, 432*(7016), 459-460. https://doi.org/10.1038/432459a.

Cluis, D., Couture, P., Bégin, R., & Visser, S. A. (1988). Potential eutrophication assessment in rivers; relationship between produced and exported loads. *Swiss Journal of Hydrology, 50*(2), 166-181. https://doi.org/10.1007/bf02538984.

Creutz, M., Van Bocxlaer, B., Abderamane, M., & Verschuren, D. (2016). Recent environmental history

of the desert oasis lakes at Ounianga Serir, Chad. *Journal of Paleolimnology, 55*(2), 167-183. https://doi.org/10.1007/s10933-015-9874-y.

Daryanto, S., Wang, L. X., & Jacinthe, P. A. (2017). Meta-Analysis of Phosphorus Loss from No-Till Soils. *Journal of Environmental Quality, 46*(5), 1028-1037. https://doi.org/10.2134/jeq2017.03.0121.

Dörnhöfer, K., & Oppelt, N. (2016). Remote sensing for lake research and monitoring – Recent advances. *Ecological Indicators, 64*, 105-122. https://doi.org/10.1016/j.ecolind.2015.12.009.

Duan, H., Ma, R., Xu, X., Kong, F., Zhang, S., Kong, W., et al. (2009). Two-Decade Reconstruction of Algal Blooms in China's Lake Taihu. *Environmental Science & Technology, 43*(10), 3522-3528. https://doi.org/10.1021/es8031852.

Fathi, A. A., & Flower, R. J. (2005). Water quality and phytoplankton communities in Lake Qarun (Egypt). *Aquatic Sciences, 67*(3), 350-362. https://doi.org/10.1007/s00027-005-0777-2.

Habeck-Fardy, A., & Nanson, G. C. (2014). Environmental character and history of the Lake Eyre Basin, one seventh of the Australian continent. *Earth-Science Reviews, 132*, 39-66. https://doi.org/10.1016/j.earscirev.2014.02.003.

Heller, M. I., Wuttig, K., & Croot, P. L. (2016). Identifying the Sources and Sinks of CDOM/FDOM across the Mauritanian Shelf and Their Potential Role in the Decomposition of Superoxide (O2-). *Frontiers in Marine Science, 3*. https://doi.org/10.3389/fmars.2016.00132.

Jin, X. C., Xu, Q. J., & Huang, C. Z. (2005). Current status and future tendency of lake eutrophication in China. *Science in China Series C-Life Sciences, 48*, 948-954.

Kislik, C., Dronova, I., & Kelly, M. (2018). UAVs in Support of Algal Bloom Research: A Review of Current Applications and Future Opportunities. *Drones, 2*(4), 35. https://doi.org/10.3390/drones2040035.

Kutser, T., Pierson, D. C., Tranvik, L., Reinart, A., Sobek, S., & Kallio, K. (2005). Using Satellite Remote Sensing to Estimate the Colored Dissolved Organic Matter Absorption Coefficient in Lakes. *Ecosystems, 8*(6), 709-720. https://doi.org/10.1007/s10021-003-0148-6.

Le, C., Zha, Y., Li, Y., Sun, D., Lu, H., & Yin, B. (2010). Eutrophication of Lake Waters in China: Cost, Causes, and Control. *Environmental Management, 45*(4), 662-668. https://doi.org/10.1007/s00267-010-9440-3.

Li, J., Yu, Q., Tian, Y. Q., Becker, B. L., Siqueira, P., & Torbick, N. (2018). Spatio-temporal variations of CDOM in shallow inland waters from a semi-analytical inversion of Landsat-8. *Remote Sensing of Environment, 218*, 189-200. https://doi.org/10.1016/j.rse.2018.09.014.

Li, J., Zhu, T., Mao, X., & Adeloye, A. J. (2016). Modeling crop water consumption and water productivity in the middle reaches of Heihe River Basin. *Computers and Electronics in Agriculture, 123*, 242-255. https://doi.org/10.1016/j.compag.2016.02.021.

Liu, Z., Meng, Y., Cai, M., & Zhou, J. (2017). Coupled effects of mulching and nitrogen fertilization on crop yield, residual soil nitrate, and water use efficiency of summer maize in the Chinese Loess Plateau. *Environmental Science and Pollution Research, 24*(33), 25849-25860. https://doi.org/10.1007/s11356-017-0194-9.

Luo, L., Ma, W., Zhao, W., Zhuang, Y., Zhang, Z., Zhang, M., et al. (2018). UAV-based spatiotemporal

thermal patterns of permafrost slopes along the Qinghai–Tibet Engineering Corridor. *Landslides, 15*(11), 2161–2172. https://doi.org/10.1007/s10346-018-1028-7.

Luo, L., Zhuang, Y., Zhao, W., Duan, Q., & Wang, L. (2020). The hidden costs of desert development. *Ambio, 49*(8), 1412-1422. https://doi.org/10.1007/s13280-019-01287-7.

Ojwang, W. O., Obiero, K. O., Donde, O. O., Gownaris, N., Pikitch, E. K., Omondi, R., et al. (2016). Lake Turkana: World's Largest Permanent Desert Lake (Kenya). In *The Wetland Book* (pp. 1-20).

Para, J., Charriere, B., Matsuoka, A., Miller, W. L., Rontani, J. F., & Sempere, R. (2013). UV/PAR radiation and DOM properties in surface coastal waters of the Canadian shelf of the Beaufort Sea during summer 2009. *Biogeosciences, 10*(4), 2761-2774. https://doi.org/10.5194/bg-10-2761-2013.

Peter, K. D., d'Oleire-Oltmanns, S., Ries, J. B., Marzolff, I., & Ait Hssaine, A. (2014). Soil erosion in gully catchments affected by land-levelling measures in the Souss Basin, Morocco, analysed by rainfall simulation and UAV remote sensing data. *Catena, 113*, 24-40. https://doi.org/10.1016/j.catena.2013.09.004.

Rose, K. C., Hamilton, D. P., Williamson, C. E., McBride, C. G., Fischer, J. M., Olson, M. H., et al. (2014). Light attenuation characteristics of glacially-fed lakes. *Journal of Geophysical Research-Biogeosciences, 119*(7), 1446-1457. https://doi.org/10.1002/2014jg002674.

Slonecker, E. T., Jones, D. K., & Pellerin, B. A. (2016). The new Landsat 8 potential for remote sensing of colored dissolved organic matter (CDOM). *Marine Pollution Bulletin, 107*(2), 518-527. https://doi.org/10.1016/j.marpolbul.2016.02.076.

Song, K., Shang, Y., Wen, Z., Jacinthe, P.-A., Liu, G., Lyu, L., et al. (2019). Characterization of CDOM in saline and freshwater lakes across China using spectroscopic analysis. *Water Research, 150*, 403-417. https://doi.org/10.1016/j.watres.2018.12.004.

Souza, V., Espinosa-Asuar, L., Escalante, A. E., Eguiarte, L. E., Farmer, J., Forney, L., et al. (2006). An endangered oasis of aquatic microbial biodiversity in the Chihuahuan desert. *Proceedings of the National Academy of Sciences, 103*(17), 6565-6570. https://doi.org/10.1073/pnas.0601434103.

Steinman, A. D., Cardinale, B. J., Munns, W. R., Ogdahl, M. E., Allan, J. D., Angadi, T., et al. (2017). Ecosystem services in the Great Lakes. *Journal of Great Lakes Research, 43*(3), 161-168. https://doi.org/10.1016/j.jglr.2017.02.004.

Su, Y., Yang, R., Liu, W., Yang, X., & Wang, M. (2014). Irrigation Water Requirement Based on Soil Conditions in a Typical Irrigation District in a Marginal Oasis. *Scientia Agricultura Sinica, 47*(6), 1128-1139. https://doi.org/10.3864/j.issn.0578-1752.2014.06.009.

Su, Y. Z., Yang, R., Liu, W. J., & Wang, X. F. (2010). Evolution of Soil Structure and Fertility After Conversion of Native Sandy Desert Soil to Irrigated Cropland in Arid Region, China. *Soil Science, 175*(5), 246-254. https://doi.org/10.1097/SS.0b013e3181e04a2d.

Templin, T., Popielarczyk, D., & Kosecki, R. (2017). Application of Low-Cost Fixed-Wing UAV for Inland Lakes Shoreline Investigation. *Pure and Applied Geophysics, 175*(9), 3263-3283. https://doi.org/10.1007/s00024-017-1707-7.

Valerio, A. D., Kampel, M., Vantrepotte, V., Ward, N. D., Sawakuchi, H. O., Less, D. F. D., et al. (2018). Using CDOM optical properties for estimating DOC concentrations and pCO(2) in the Lower Amazon River. *Optics Express, 26*(14), A657-A677. https://doi.org/10.1364/Oe.26.00a657.

Wang, Q., Li, F., Zhao, L., Zhang, E., Shi, S., Zhao, W., et al. (2010). Effects of irrigation and nitrogen application rates on nitrate nitrogen distribution and fertilizer nitrogen loss, wheat yield and nitrogen uptake on a recently reclaimed sandy farmland. *Plant and Soil, 337*(1-2), 325-339. https://doi.org/10.1007/s11104-010-0530-z.

Wells, M. L., Trainer, V. L., Smayda, T. J., Karlson, B. S. O., Trick, C. G., Kudela, R. M., et al. (2015). Harmful algal blooms and climate change: Learning from the past and present to forecast the future. *Harmful Algae, 49*, 68-93. https://doi.org/10.1016/j.hal.2015.07.009.

Wen, J., Su, Z., Zhang, T., Tian, H., Zeng, Y., Liu, R., et al. (2014). New evidence for the links between the local water cycle and the underground wet sand layer of a mega-dune in the Badain Jaran Desert, China. *Journal of Arid Land*. https://doi.org/10.1007/s40333-014-0062-0.

Wu, D., Li, R., Zhang, F., & Liu, J. (2019). A review on drone-based harmful algae blooms monitoring. *Environmental Monitoring and Assessment, 191*(4). https://doi.org/10.1007/s10661-019-7365-8.

Xie, Y. W., Wang, G. S., Wang, X. Q., & Fan, P. L. (2017). Assessing the evolution of oases in arid regions by reconstructing their historic spatio-temporal distribution: a case study of the Heihe River Basin, China. *Frontiers of Earth Science, 11*(4), 629-642. https://doi.org/10.1007/s11707-016-0607-y.

Yang, R., & Liu, W. J. (2010). Nitrate contamination of groundwater in an agroecosystem in Zhangye Oasis, Northwest China. *Environmental Earth Sciences, 61*(1), 123-129. https://doi.org/10.1007/s12665-009-0327-7.

Yang, R., Su, Y.-z., Wang, T., & Yang, Q. (2016). Effect of chemical and organic fertilization on soil carbon and nitrogen accumulation in a newly cultivated farmland. *Journal of Integrative Agriculture, 15*(3), 658-666. https://doi.org/10.1016/s2095-3119(15)61107-8.

Zhang, Y., Zhao, W., Ochsner, T. E., Wyatt, B. M., Liu, H., & Yang, Q. (2019). Estimating Deep Drainage Using Deep Soil Moisture Data under Young Irrigated Cropland in a Desert-Oasis Ecotone, Northwest China. *Vadose Zone Journal, 18*(1), 180189. https://doi.org/10.2136/vzj2018.10.0189.

Zhang, Y., Zhou, Y., Shi, K., Qin, B., Yao, X., & Zhang, Y. (2018). Optical properties and composition changes in chromophoric dissolved organic matter along trophic gradients: Implications for monitoring and assessing lake eutrophication. *Water Research, 131*, 255-263. https://doi.org/10.1016/j.watres.2017.12.051.

Zhao, J., Cao, W., Wang, G., Yang, D., Yang, Y., Sun, Z., et al. (2009). The variations in optical properties of CDOM throughout an algal bloom event. *Estuarine, Coastal and Shelf Science, 82*(2), 225-232. https://doi.org/10.1016/j.ecss.2009.01.007.

Zhao, W., & Chang, X. (2014). The effect of hydrologic process changes on NDVI in the desert-oasis ecotone of the Hexi Corridor. *Science China Earth Sciences, 57*(12), 3107-3117. https://doi.org/10.1007/s11430-014-4927-z.

Zhao, W., Liu, B., & Zhang, Z. (2010). Water requirements of maize in the middle Heihe River basin, China. *Agricultural Water Management, 97*(2), 215-223. https://doi.org/10.1016/j.agwat.2009.09.011.

Table 1. Flight- and yield-related ground data acquisition schedule in 2018. N represents the measurement number of the water quality sensor.

ID	Date	Growth stage	Weather	Altitude	N	Photos	GSD
1	May 22	Flowering	Clear	50 m	38	949	2.18 cm
2	July 29	Mid-grain filling	Clear	120 m	52	324	3.36 cm
3	September 19	Maturity	Clear	120 m	20	371	3.03 cm

Table 2. Lake area and water level changes, average quality of sampled lake water and simulated CDOM absorption coefficient in different crop growth stages (mean ± SD). *significant ($P < 0.05$) differences for water quality sampling indicated between flowering (1), mid-grain filling (2), and maturity (3) are in superscript, while there is a significant ($P < 0.05$) correlation for CDOM absorption coefficient during the three growth stages. NS = not significant ($P > 0.05$).

	Flowering	**Mid-grain filling**	**Maturity**
	May 22	July 29	September 19
Lake Area (m^2)	61719	56382	78808
Water Level (m)	1330.37	1329.33	1331.79
Conductivity (mS/cm)	$750.08 \pm 80.32^{*2,3}$	$825.54 \pm 39.85^{*1,3}$	$729.92 \pm 35.65^{*1,2}$
DO (mg/L)	$6.93 \pm 1.27^{*3}$	$6.73 \pm 1.34^{*3}$	$9.40 \pm 1.02^{*1,2}$
fDOM (ppb QSE)	$5.28 \pm 2.53^{*2,3}$	$9.51 \pm 7.40^{*1,3}$	$6.27 \pm 1.67^{*1,2}$
ORP (mV)	$-275.27 \pm 31.89^{*2,3}$	$-121.13 \pm 47.49^{*1,3}$	$-431.78 \pm 34.16^{*1,2}$
pH	$9.27 \pm 0.15^{*3}$	$9.36 \pm 0.20^{*3}$	$10.32 \pm 0.45^{*1,2}$
Salinity (psu)	0.41±0.04	0.43±0.02	0.40±0.02
CDOM absorption coefficient (m^{-1})	$1.88 \pm 0.96^{*2}$	$5.81 \pm 0.99^{*1}$	3.75 ± 0.33^{NS}

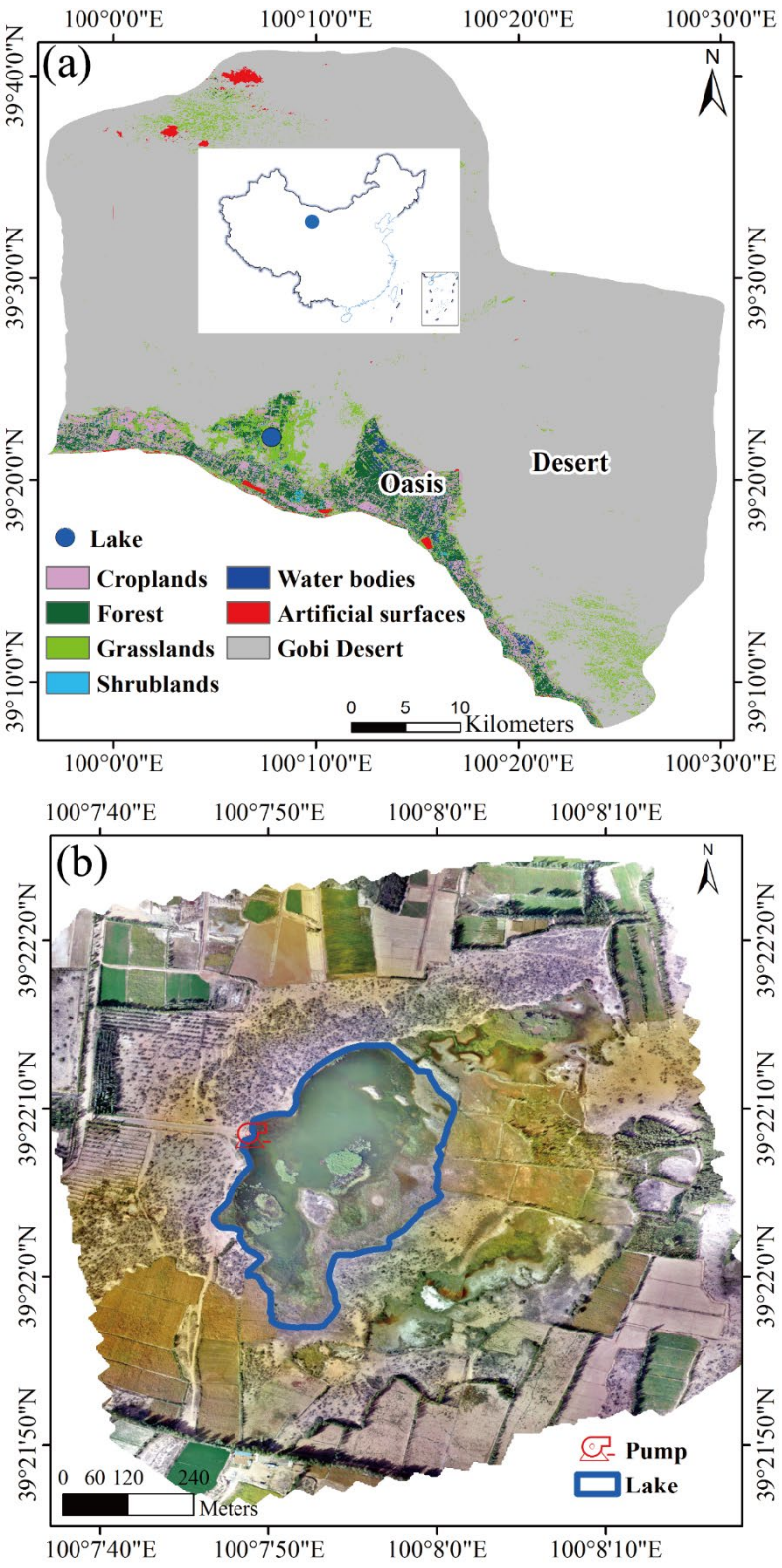

Figure 1. Maps showing the location of the study area. (a) Location of Suolongtan Lake (solid blue circle) in relation to the oasis. (b) Mosaic visual image of Suolongtan Lake (blue line) and its surroundings.

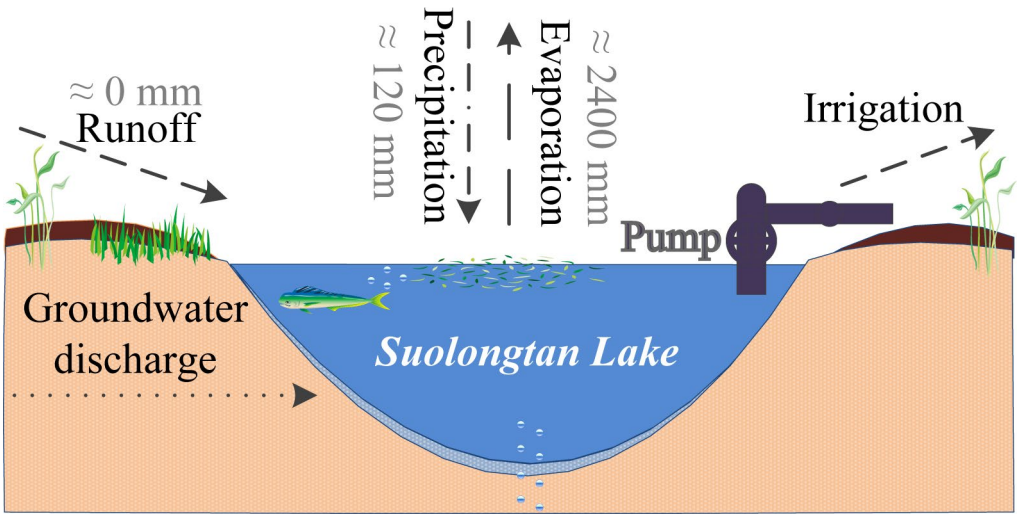

Figure 2. Summary of the hydrological processes in Suolongtan Lake, China.

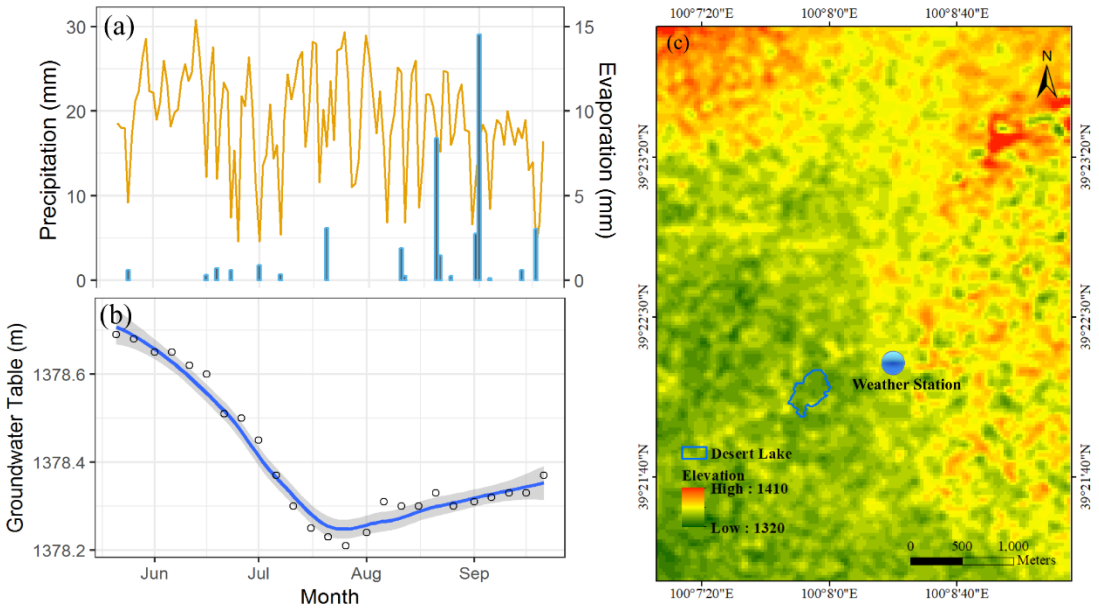

Figure 3. Precipitation, evaporation and groundwater tables at weather stations near the study area and elevation around the desert lake. (a) Daily precipitation (bar chart) and evaporation (curve) from 22 May 2018 to 19 September 2018; (b) groundwater table every five days from 21 May 2018 to 21 September 2018; (c) elevation around the lake.

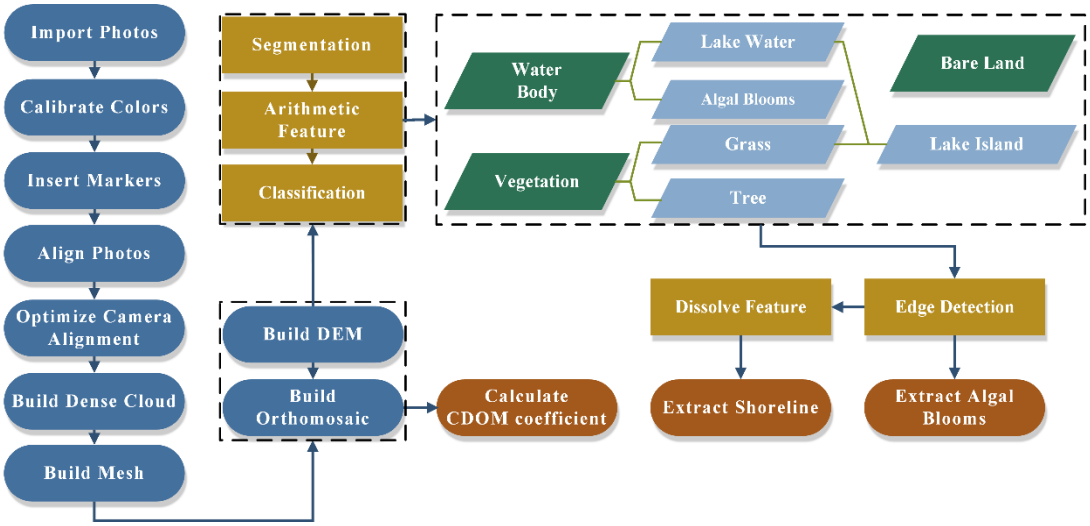

Figure 4. Workflow for processing UAV imagery.

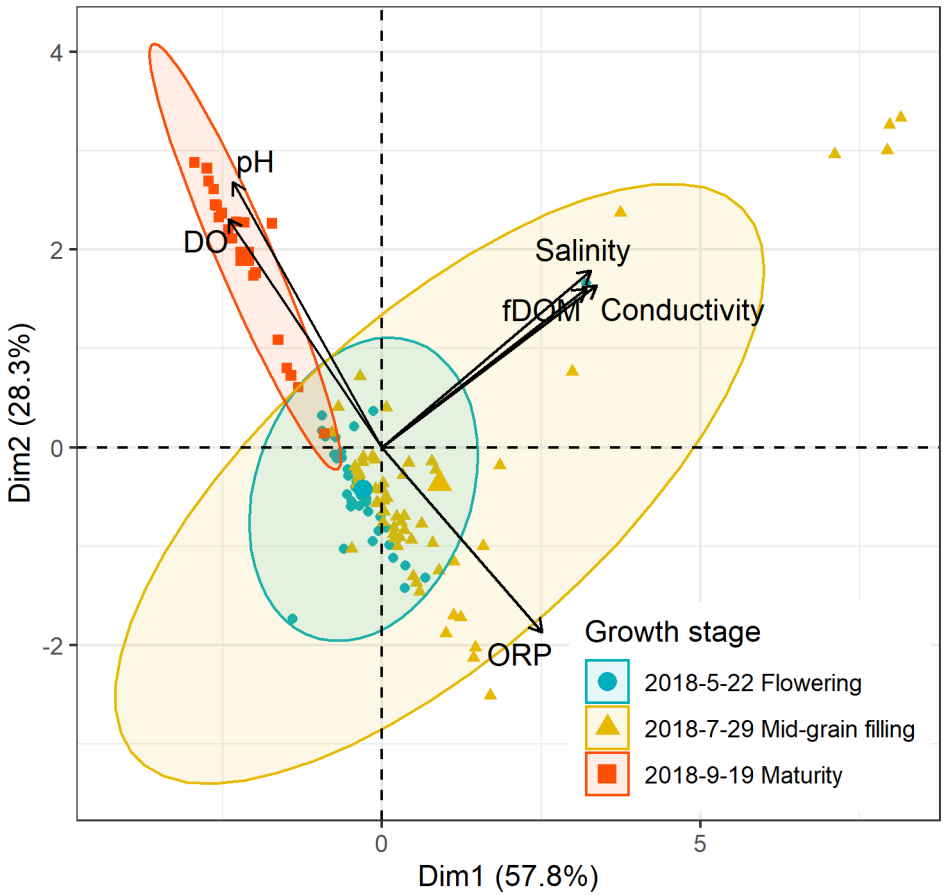

Figure 5. PCA score plot of water quality parameters at different stages of crop growth.

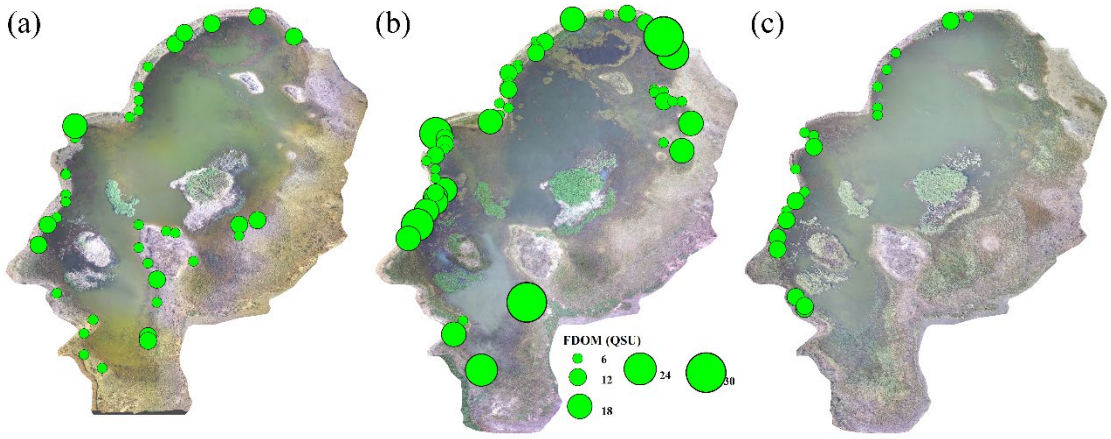

Figure 6. Spatial distribution of fDOM in the lake at different crop growth stages. (a) Flowering; (b) Mid-grain filling; (c) Maturity.

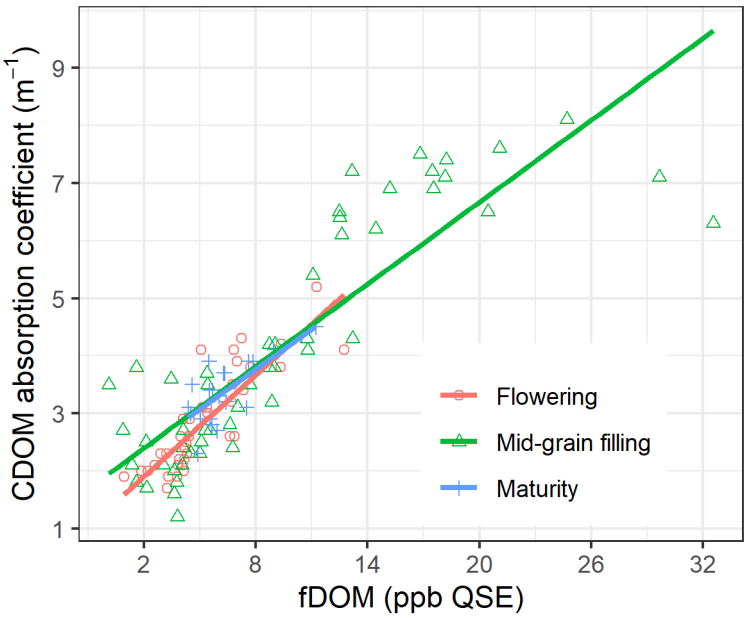

Figure 7. The relationship between fDOM and the estimated CDOM absorption coefficient at different crop growth stages.

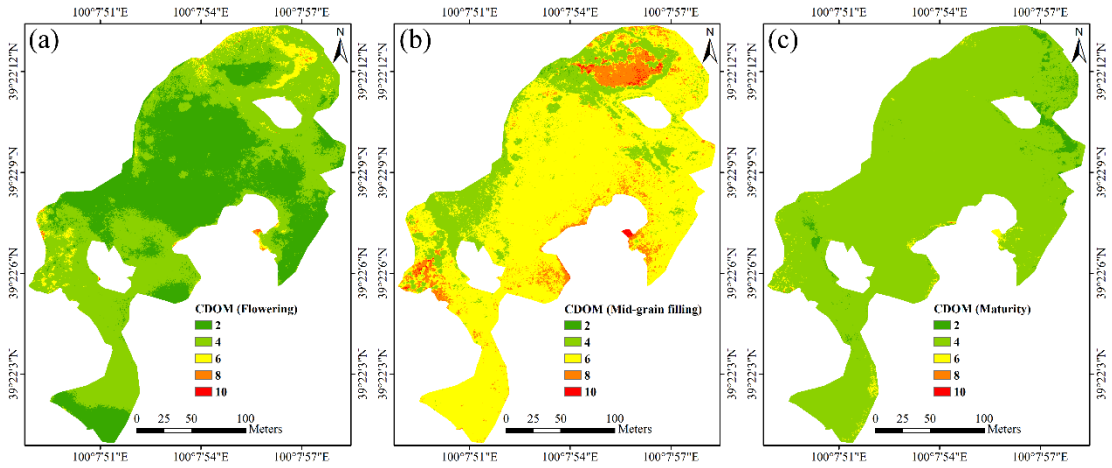

Figure 8. Spatial changes in the simulated CDOM absorption coefficient of the lake at different crop growth stages. (a) Flowering; (b) Mid-grain filling; (c) Maturity.

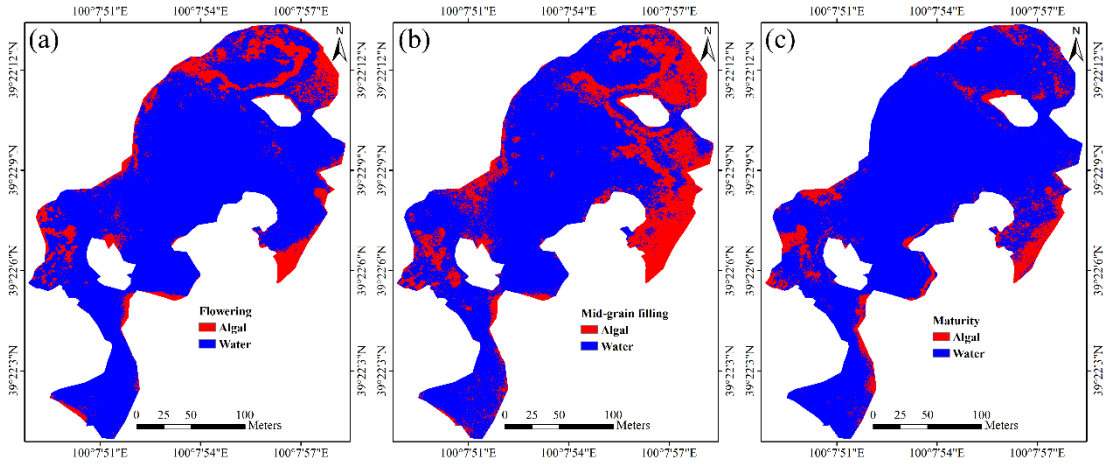

Figure 9. Spatial distribution of algal blooms in the lake at different crop growth stages. (a) Flowering; (b) Mid-grain filling; (c) Maturity.

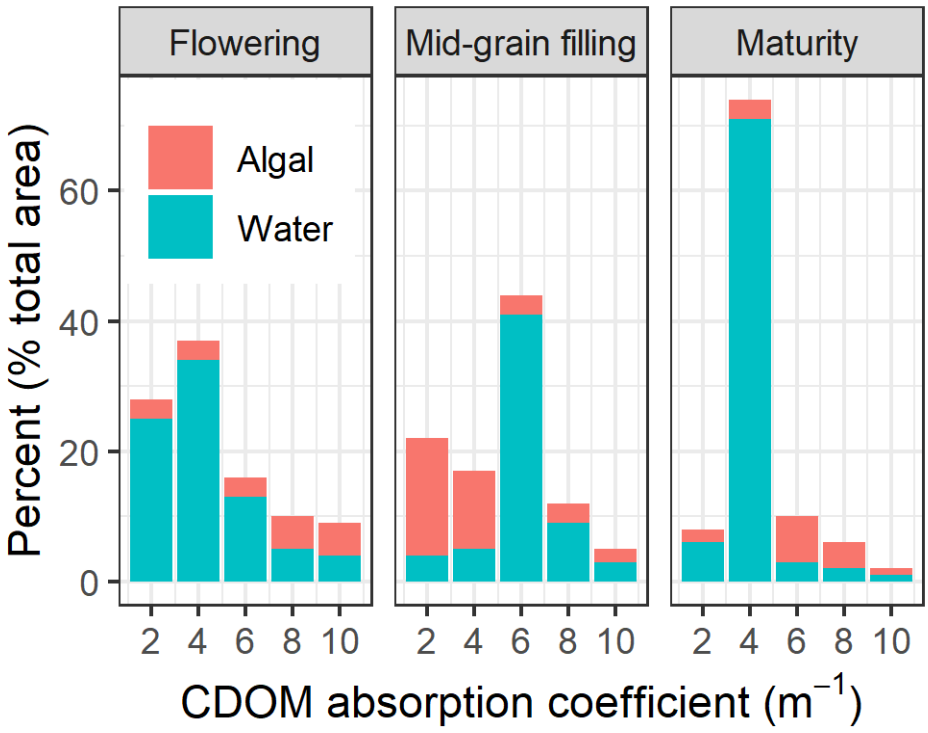

Figure 10. Percentages of algal bloom area (algal) and nonalgal boom area (water) to total area for different CDOM absorption coefficients under different crop growth stages.